Climate Dynamics (1990) 4:157-174

Climate Dynamics

Northern Hemisphere atmospheric response to changes of Atlantic Ocean SST on decadal time scales: a GCM experiment*

Andreas Hense[1], Rita Glowienka-Hense[1], Hans von Storch[2], and Ursula Stähler[3]

[1] Alfred-Wegener Institut für Polar- und Meeresforschung, Am Handelshafen 12, D-2850 Bremerhaven, Federal Republic of Germany
[2] Max Planck Institut für Meteorologie, D-2000 Hamburg, Federal Republic of Germany
[3] Institut für Geophysik und Meteorologie, Universität Frankfurt, D-6000 Frankfurt, Federal Republic of Germany

Received November 2, 1989/Accepted June 18 1990

Abstract. Analyses indicate that the Atlantic Ocean sea-surface temperature (SST) was considerably colder at the beginning than in the middle of the century. In parallel, a systematic change in the North Atlantic sea-level pressure (SLP) pattern was observed. To find out whether the SST and SLP changes analyzed are consistent, which would indicate that the SST change was real and not an instrumental artifact, a response experiment with a low-resolution (T21) atmospheric GCM was performed. Two perpetual January simulations were conducted, which differ solely in the Atlantic Ocean (40° S–60° N) SST: the "cold" simulation utilizes the SSTs for the period 1904–1913; the "warm" simulation uses the SSTs for the period 1951–1960. Also, a "control" run with the model's standard SST somewhat between the "cold" and "warm" SST was made. For the response analysis, a rigorous statistical approach was taken. First, the null hypothesis of identical horizontal distributions was subjected to a multivariate significance test. Second, the level of recurrence was estimated. The multivariate statistical approaches are based on hierarchies of test models. We examined three different hierarchies: a scale-dependent hierarchy based on spherical harmonics (S), and two physically motivated ones, one based on the barotropic normal modes of the mean 300 hPa flow (B) and one based on the eigenmodes of the advection diffusion operator at 1000 hPa (A). The intercomparison of the "cold" and "warm" experiments indicates a signal in the geostrophic stream function that in the S-hierarchy is significantly nonzero and highly recurrent. In the A-hierarchy, the low level temperature field is identified as being significantly and recurrently affected by the altered SST distribution. The SLP signal is reasonably similar to the SLP change observed. Unexpectedly, the upper level streamfunction signal does not appear to be significantly nonzero in the B-hierarchy. If, however, the pairs of experiments "warm versus control" and "cold versus control" are examined in the B-hierarchy, a highly significant and recurrent signal emerges. We conclude that the "cold versus warm" response is not a "small disturbance" that would allow the signal to be described by eigenmodes of the linear system. An analysis of the three-dimensional structure of the signal leads to the hypothesis that two different mechanisms are acting to modify the model's mean state. At low levels, local heating and advection are dominant, but at upper levels the extratropical signal is a remote responce to modifications of the tropical convection.

Introduction

Decadal changes of North Atlantic SST and SLP

The time series of Atlantic Ocean sea-surface temperatures (SST) shows marked large-scale low-frequency variations in decadal time scales (Höflich 1974). This is exemplified by the dominant first two empirical orthogonal functions (EOFs) of SST in January (Fig. 1a, b) and their amplitudes from 1860 to 1960 (Fig. 1c, d). Both the patterns and the amplitudes for the other months are very similar to the January patterns and amplitudes. The pattern of the first EOF implies that its amplitude is related to an area average of the anomalous SST field over the Atlantic between 70° N and 40° S. A period of anomalous low temperatures is observed from the beginning of the century until around 1920 while a period of positive temperature anomalies is found between 1950 and 1960. There is evidence that these changes are not an instrumental artifact but are in part real: the HSST ["historical sea-surface temperature"; Höflich (1974)] data set is fairly homogeneous, as it includes only bucket reports. Also, similar tempera-

* This paper was presented at the International Conference on Modelling of Global Climate Change and Variability, held in Hamburg 11–15 September 1989 under the auspices of the Meteorological Institute of the University of Hamburg and the Max Planck Institute for Meteorology. Guest Editor for these papers is Dr. L. Dümenil.
AWI Publication no. 254

Offprint requests to: A Hense

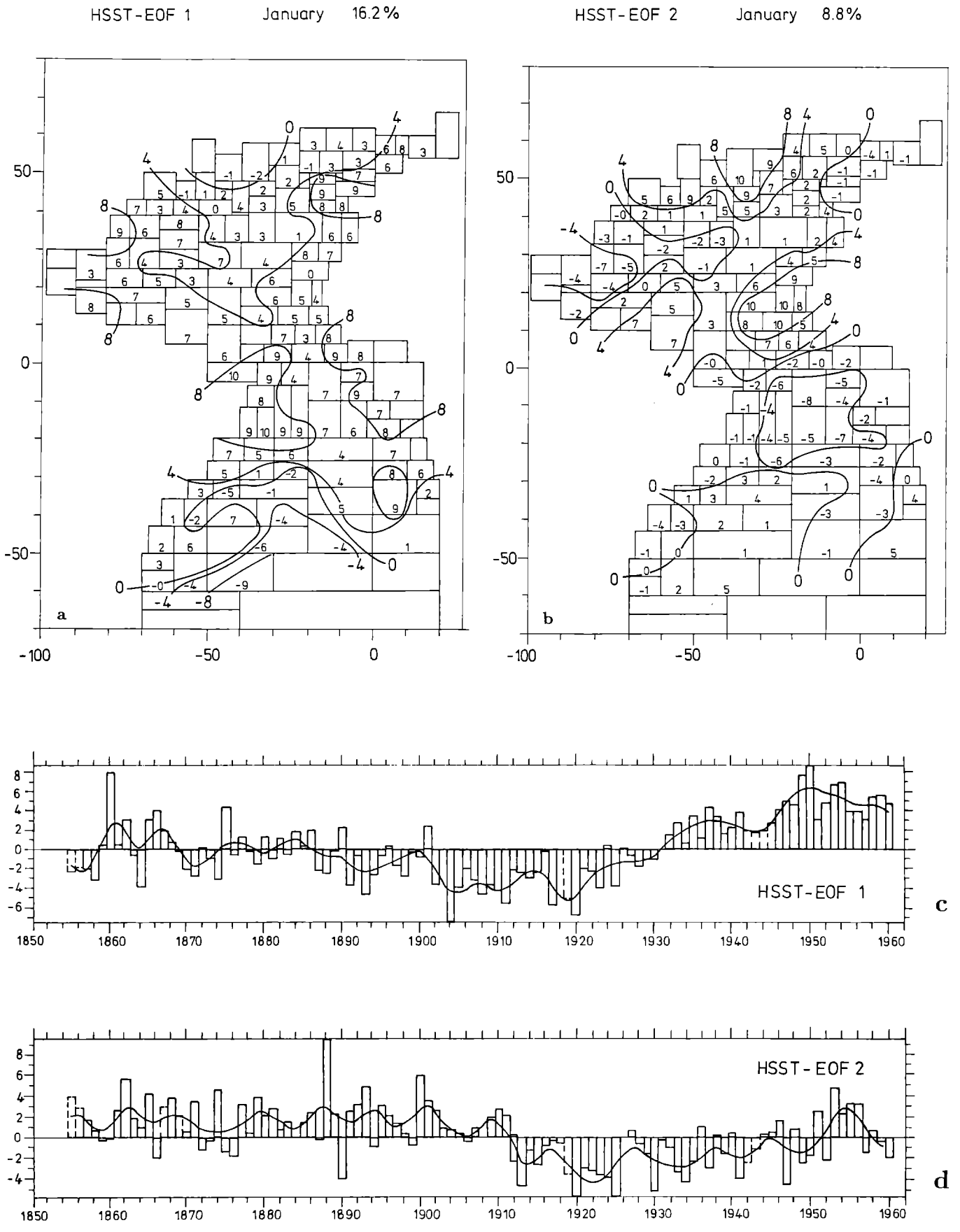

Fig. 1a–c. The first two January, EOFs of the historical sea-surface temperature (HSST: Höflich 1974). **a** EOF1 (16%); **b** EOF2 (9%). Pattern of EOFs is normalized to have an absolute maximum value of 10; *contour lines* are drawn in subjectively for better visualization. **c** Time amplitude of EOF1; **d** time amplitude of EOF2

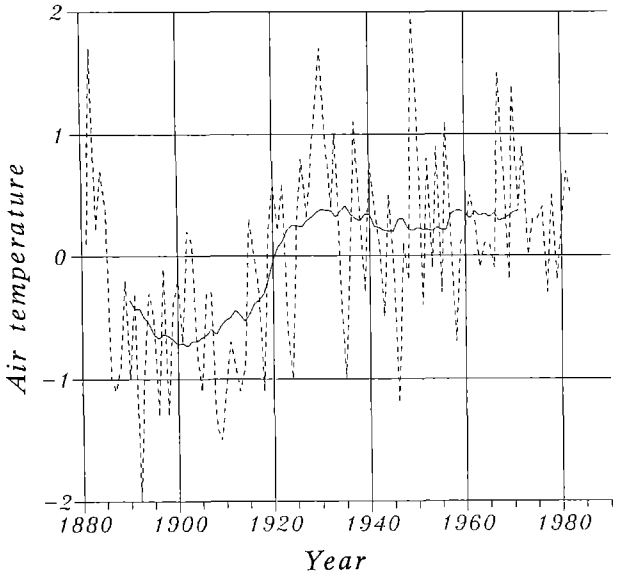

Fig. 2. Observed air-temperature anomaly in January at Funchal (Madeira). After the World Meteorological Station Climatology. According to Jones et al. (1985), the time series does not suffer from inhomogeneities. *Dashed line:* raw data; *continous line:* 10-year running mean. Units: °C

ture changes are reflected in air temperature records at Funchal on Madeira (Fig. 2).

Parallel to these oceanic changes, changes in the atmosphere have also been observed, in particular in the January sea-level pressure (SLP) field over the North Atlantic. This is demonstrated in Fig. 3, which shows the (filtered, see below) decadal mean difference between surface pressure in the beginning and in the middle of the present century. This difference exhibits a large-scale and coherent signal over the whole Atlantic-European sector (see discussion below).

The questions to be asked are:

1. Are the changes real or artificial due to instrumental inhomogeneities and insufficient sampling?
2. Are the atmospheric changes a response to changed oceanic conditions or vice versa?

If we can further establish a reasonable agreement between observed and simulated decadal changes, one may also conclude that the T21 climate is probably good enough to infer conclusions from the model to the real atmosphere.

General approach

A first attempt to find an answer to the above questions through the help of a model study is reported in this paper. Three extended general circulation model (GCM) runs were performed, each using a different SST distribution in the Atlantic Ocean. One run was done with the model's standard SST that is typical for the 1970s and two runs with the distributions averaged for the above-mentioned decades: 1903–1914 and 1951–1960. Because of computer-time limitations, the experiments are performed in the "permanent January

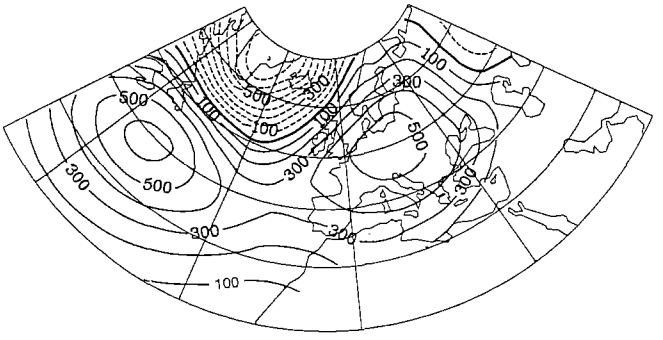

Fig. 3. Significant and recurrent signal in the difference between the observed sea-level pressure decadal means January 1904–13 and 1951–60. Units: 10^{-2} hPa; contour interval 1 hPa. Negative anomalies are *dashed*

mode". The first experiment is called "control" and the other two "cold" and "warm". We are aware that the omission of the annual cycle may restrict the comparison with observations since one can expect different responses when imposing a steady anomalous forcing onto a steady background instead of onto a seasonal varying background (Zwiers and Boer 1987).

The expected result is that the differences between the atmospheric circulation in the GCM experiments are comparable to the observed changes. Systematic model errors have a non-neglible component on the "broad pattern" of the atmosphere; therefore, the coincidence of the observations and of the GCM simulations will be only in their broad pattern.

It is well known that in this type of GCM sensitivity experiments the signal is often masked by the strong "weather noise" at midlatitudes. Therefore, it is inappropriate to compare naively the observed decadal change and the mean simulated difference "cold minus warm". Instead, the stochastic character of the random variable "January mean flow" must be taken into consideration by testing the null hypothesis:

"The simulated patterns of the hemispheric winter circulation associated with anomalous low and high Atlantic SSTs are identical."

If such a statistical test yields the positive result of a nonzero signal (i.e., the rejection of the null hypothesis), the following questions regarding the physics of the signal must be asked:

1. Is the response statistically stable, i.e., is it associated with a large probability of appearance in individual January means?
2. What is the three-dimensional structure of the signal?
3. Can we specify reduced models that allow us to understand the modelled changes in terms of simplifying physical theory?

The last question and the test of the null hypothesis mentioned above may conveniently be treated jointly. Since the random variable "January mean flow" is a vector random variable, a multivariate statistical test must be used (Hasselmann 1979). This may be done in terms of a series of tests (Barnett et al. 1981) using a hierarchy for "guess patterns" that are specified prior

to the test without using information from the GCM experiments except the time mean fields. The GCM fields are projected onto the guess patterns and the test is done in the low-dimensional subspace spanned by the guess patterns. The rejection of the null hypothesis is a statistical proof that the guess patterns are useful in explaining the model's response.

Studies that have used the guess pattern/hierarchy approach successfully have been published by Hannoschöck and Frankignoul (1985), Hense (1986), Storch and Kruse (1985), Frankignoul and Molin (1988a, b) and Lautenschlager et al. (1988). They have primarily used scale arguments to specify the guess patterns, i.e., surface spherical harmonics or, with little success, the response of physical models linearized around a zonally symmetric basic state. In the present study, in addition to the problem-independent surface-spherical harmonics, we use two physically motivated sets of guess patterns: the eigenfunctions of the barotropic vorticity equation linearized around the (zonally nonsymmetric) mean state for explaining the anomalies in the upper troposphere and the eigenmodes of the advection-diffusion operator for the flow at 1000 hPa for explaining the temperature response of the layer 850/1000 hPa.

The question of the statistical stability of the response may be adressed by the concept of "recurrence analysis" (von Storch and Zwiers 1988; Zwiers and von Storch 1989). We use both the univariate "local" recurrence analysis and the pattern-oriented multivariate "global" analysis.

After having found a significant "cold versus warm" signal, it is an interesting question to ask if the signal depends linearly on SST forcing. We may address this question by examining experiments "cold versus control" and "warm versus control" that operate with the same SST anomaly pattern. For "cold vs control" the intensity of the SST anomaly is strongly negative, and for "warm vs control" it is moderately positive. The analyses of the "cold vs control" and "warm vs control" experiments are done in the same manner as the "cold vs warm" analysis.

Purpose and organization of the study

The purpose of the paper is threefold:

1. To demonstrate the consistency of observed changes in SST and SLP on decadal time scales and to show that the observed SLP changes may partially be understood as atmospheric response to changing boundary conditions (SST)
2. To show the usefulness of reduced models to interpret the output of GCMs, which usually have as complex a behavior as the real atmosphere
3. To study the linearity of the atmospheric response to large-scale SST anomalies

We do not consider two related questions in this paper: the abrupt change of temperature in the northern part of the North Atlantic (e.g., van Loon and Rogers 1978; Rogers 1985) and the slow increase of interannual variability from the beginning to the middle of the present century (van Loon and Madden 1983). Our SST data set do not resolve the northern part of the North Atlantic so that information on SST in that area is not available. To address the variability problem the horizontal resolution (T21) of the GCM is likely to be too coarse.

The paper is organized as follows. In section 2 the GCM and the experiments with it are described; in section 3 the general statistical approach is briefly summarized. The hierarchies of guess patterns and their physical motivation are presented in section 4. The filtering of the statistically significant signal in the "cold vs warm" experiment, its physical plausibility and its statistical stability are presented in section 5. The linearity of the model's response to anomalous Atlantic SST is examined in section 6. The physics of the identified signal are discussed in the final section – section 7.

Data

GCM experiments

The Hamburg version of the low-resolution ECMWF T21 atmospheric GCM was used to perform the experiments. For details of the structure, physics and general performance of the model, see Fischer (1987) and von Storch (1988). The perpetual January model runs were identical except for the prescribed SST field in the Atlantic between 70° N and 35° S. The first run was integrated over 13 months ("control") using the model's standard SST climatology of Alexander and Mobley (1976), which is representative for the 1970s. The other two runs, named "warm" and "cold", were integrated over 24 months each and used the January Atlantic SST averaged over the decades 1904–1913 ("cold") and 1951–1960 ("warm"). The first month in each run was considered as the spin-up phase needed by the model to reach its equilibrium.

The Atlantic SST fields were derived from the irregularly spaced HSST data set (Höflich 1974) by an EOF analysis. EOFs and their amplitudes have been calculated from the January SST. The first two EOFs (Fig. 1) that explain 25% of the total interannual variance were considered relevant in describing the decadal changes. Therefore, the anomaly distribution described by the first two EOFs was reconstructed and, after decadal averaging, used as an anomalous boundary condition. Figure 4 shows the resulting difference between the "cold" and "warm" SST fields. There is an anomaly of 1.2° C in the tropical Atlantic and a structured anomaly between 1 and 0.3° C in the North Atlantic while a negative anomaly occurs in the South Atlantic. The "cold vs control" ("warm vs control") SST anomaly is roughly two thirds (one third) of the "cold vs warm" anomaly. The SST anomaly patterns in the "cold vs control" and "warm vs control" experiments are identical and are broadly similar to that in "cold vs warm".

Verification data

No upper-air data are available from the first decades of this century, so the verification of the GCM results is limited to SLP, which is available to us for the period from 1881 to 1984. The different data sources and errors in this SLP data have been discussed by Glowienka (1985). Time series of station data (World Meteorological Station Climatology, available at NCAR) are also available but are of limited value since the expected signal is large scale while the point measurements are likely to be influenced by local peculiarities and inhomogeneities.

Statistics

As mentioned in the Introduction, we will use statistical techniques to evaluate the GCM response in a noisy environment. We consider the 30-day mean of a certain variable, e.g., stream function at 300 hPa or sea-level pressure, as a random variable, that is, each 30-day mean obtained from the three runs, control, warm and cold, is considered to be a random sample of a random vector variable. These samples may be used to test whether the data contradict the null hypothesis of a zero signal (significance test) and to estimate the level of global or local recurrence (level of recurrence). The (multivariate) significance test and the estimation of the level of recurrence will be done in a hierarchy (guess patterns).

Significance test

The null hypothesis to be tested is:

$$H_0: \ \mu_i = \mu_j \tag{1}$$

where μ_i is the expectation of the vector random variable x_i. The index i (and j) identifies the experiment, i.e., the cold, warm or control experiment may be tested conveniently by the Hotelling H_0 statistic if one assumes that the underlying ensemble is a multivariate normal distributed one [e.g., Hannoschöck and Frankignoul (1985) or Hense (1986)]:

$$T^2 = \frac{n_i n_j}{n_i + n_j} D^2 \tag{2}$$

with

$$D^2 = (\overline{x_i} - \overline{x_j})^t S^{-1} (\overline{x_i} - \overline{x_j}) \tag{3}$$

Here, the sample mean of experiment i is denoted by $\overline{x_i}$. S is the pooled estimate of the variance/covariance matrix Σ, and n_i the number of independent samples available from experiment i. To get an invertible S the dimension of the random variable, d, has to be smaller than the total number of available independent samples, $n_i + n_j - 2$.

If H_0 is true, the function

$$F = \frac{n_i + n_j - d - 1}{d(n_i + n_j - 2)} T^2 \tag{4}$$

is Fisher-F distributed with d and $n_i + n_j - d - 1$ degrees of freedom: If F exceeds the $(1-\alpha)$ quantile of the Fisher-F distribution, H_0 may be rejected at a risk of α. That is the probability to observe such a large F by chance if $\mu_i = \mu_j$ is less than α.

Estimation of the level of recurrence

The rejection of the null hypothesis H_0 is equivalent to the acceptance of the alternative hypothesis "$\mu_i \neq \mu_j$". It does not indicate if the signal, i.e., the difference $\mu_i - \mu_j$, is large or small. In fact, the power of the Hotelling test depends on the number of available samples, $n_i + n_j$: the more samples, the better the chances to detect a nonzero signal. In other words, "significance" is in part a property of the considered random variables, but also depends on the sample size, which has no practical consequences for the physical problem under consideration but is a characteristic of the experimental design (Fig. 5a).

If the considered random variables, x_i and x_j, are univariate and Gaussian, another view of the problem is the following. The alternative hypothesis "$\mu_i = \mu_j$ is wrong" is equivalent to the probability statement

$$P(x_j > \overline{x_i}) > q \tag{5}$$

The probability q will be large if the separation of the two variables is large, i.e., if the signal $\mu_i - \mu_j$ is physically significant. A q close to 50% is indicative that the difference is not relevant. If, however, q is, say 51% the test will reject H_0 if the sample size is large enough, that is, statistical significance is a necessary but not sufficient condition for physical significance.

This somewhat unsatisfactory situation may be overcome by "recurrence analysis" [von Storch and Zwiers (1988) and Zwiers and von Storch (1989)]. Using multivariate discriminant analysis, it is possible to define a $(d-1)$ dimensional hyperplane $\varkappa$, which divides the whole R^d in two subsets S_i and S_j such that

$$P(x_j \in S_i) = P(x_i \in S_j) \leq 1 - p \tag{6}$$

(see Fig. 5b). Since $S_i \cup S_j = R^d$, (6) is equivalent to $P(x_j \in S_j) = P(x_i \in S_i) = p$. If p is large (or small), the separation of the probability densities of the two random variables x_i and x_j is large, and if p is close to 50%, the separation is small.

In the present paper we estimate the level of recurrence "globally" in the low-dimensional subspace used for the significance test and "locally" at each grid point, after having found significantly nonzero signals with the Hotelling test. If we suppose that the two random variables x_i and x_j are normally distributed with identical covariance matrix, $x_i = N(\mu_i, \Sigma)$ and $x_j = N(\mu_j, \Sigma)$, the level of recurrence p may conveniently be estimated using the "OS method" [Zwiers and von Storch (1989); Page (1985); Okamoto (1963)]:

$$1-p=\mathrm{erf}\left(-\frac{DS}{2}\right)+\frac{\phi\left(-\frac{DS}{2}\right)}{(n_i+n_j-2)}\left(\frac{DS}{16}\left(\frac{(n_i+n_j-1)^2-1)}{n_i n_j}\right)-\frac{d-1}{4DS}\left(\frac{(n_i-3n_j)(n_i+n_j-2)}{n_i n_j}-DS^2\right)\right) \quad (7)$$

where ϕ denotes the Gaussian probability density function, $\mathrm{erf}(x)$ the error function, and DS^2 the "shrunken D":

$$DS^2=\frac{(n_i+n_j-d-3)}{(n_i+n_j-2)}D^2 \quad (8)$$

In the univariate case (8) is the difference of sample means measured in units of the estimated standard deviation. A level of $p=84\%$ corresponds to the well known "2σ" rule of thumb. The difference between the two means is larger than twice the standard deviation. $p=(60,66,84)\%$ in (6) corresponds to $q=(70,80,98)\%$ in (5) [von Storch and Zwiers (1988), their Table 2].

The estimation of the level of recurrence may be done without any reference to the significance of the distance of the climates, D, and any nonzero D will give a recurrence different from 0.5. However, from the arguments of the preceding section, it is clear that a certain level of recurrence is only meaningful after having rejected the null hypothesis of a zero signal with a sufficiently small risk.

Guess patterns and hierarchies of test models

The dimension of the vectors x_i and x_j considered in this study is the number of gridpoints on the northern hemisphere, i.e., of the order of 10^3. On the other hand, the numbers of independent samples, n_i and n_j, are of the order of 30. Therefore, the sample covariance matrix in gridpoint space cannot be inverted and the test statistic D^2 cannot be calculated. To overcome this problem, the data are projected into a low-dimensional subspace with dimension $d \leq 30$. The subspace is specified by a linear basis $\{g_1,\ldots g_d\}$. The high-dimensional vectors, g_k, which can be displayed as maps covering the whole northern hemisphere, are called guess patterns.

There are two advantages of the guess pattern concept that was suggested by Hasselmann (1979). First, it is possible to increase the power of the test, i.e., the probability to identify a signal confidently by selecting patterns that are à priori known or are believed to represent the signal. Second, when using indexed guesses the analysis may be done using the method of hierarchical ordering of certain à priori chosen test models (Barnett et al. 1981): The test is done sequentially on subspaces of increasing dimension $\{g_1,\ldots g_k\}$, $k \leq d$. In this way for each k one "model" is fitted to the data, namely, the projection of the full signal on the subspace spanned by the first k guesses. If the null hypothesis, which depends now on the number k and is thus labelled as H_0^k, is rejected for certain k's at an error level of 10%, we chose as the best model the one with maximum k and an estimated level of recurrence $p \simeq 80\%$.

There are essentially three strategies to derive sequences of useful guess patterns (von Storch 1987):

1. A priori information on the expected signal. This information may originate from independent observations or numerical experiments. In our case no such information is readily available.
2. Patterns that are known to be effective in representing data but are not specifically related to the problem under consideration. In this study we use surface spherical harmonics. The advantage of this specific hierarchy is that it may be applied without any restrictions to all horizontal fields generated by the GCM. For the verification study on sea-level pressure EOFs calculated for the Atlantic-European region from all January data between 1881 and 1984 are also used.
3. Patterns obtained from some simplified theory that is supposed to describe the considered problem to some extent. We use two simple models to anticipate the GCM experiment signals: the eigenfunctions of the linearized barotropic vorticity equation and the eigenmodes of the advection diffusion operator for the flow at 1000 hPa.

S-hierarchy: scale-dependent hierarchy of surface spherical harmonics

The surface spherical harmonics Y_l^m, which formally are defined as the eigenfunctions of the Laplacian on the sphere, are known to represent data on a sphere. They may conveniently be indexed by the "total" wave number l and the zonal wave number m. l is indicative of the horizontal scale of the function and m of the zonal scale. The scales decrease with increasing indices l and m.

From the scale of the anomalous forcing (Fig. 4), we anticipate that the signal will be a larger scale one. Therefore the "S-hierachy" of spherical harmonics is specified by the indices l and m [Hannoschöck and Frankignoul (1985), Hense (1986)] with the ordering according to l and, at a fixed l, with increasing zonal wave number m ($\leq l$). Thus, the large-scale modes are being tested first.

Considering hemispheric fields alone, we limit the analysis to either odd (stream function) or even (sea-level pressure, temperature) modes. Since we are interested in difference patterns and not so much in changes of the hemispheric mean, the superrotation mode Y_1^0 is disregarded.

B-Hierarchy: barotropic normal modes

The quasigeostrophic barotropic vorticity equation is supposed to model small disturbances of the midlatitude atmospheric flow to first order.

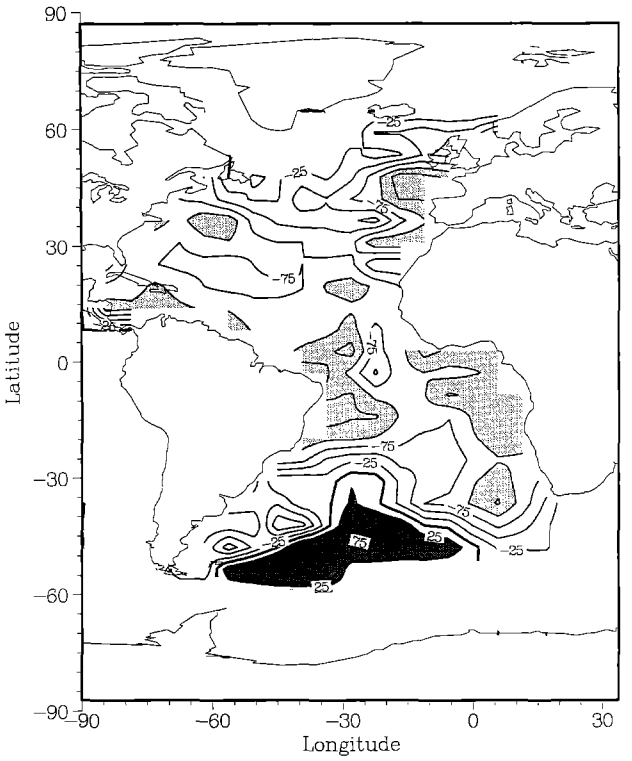

Fig. 4. Decadal difference field of the Atlantic Ocean SST in January between 1904–1913 ("cold" experiment) and 1951–1960 ("warm" experiment). The field is reconstructed from the first two January EOFs shown in Fig. 1. *Lightly shaded areas* indicate anomalies less than −1 K; *dark shaded areas* indicate anomalies larger than +0.25 K; units 10^{-2}° C; contour interval 0.25° C

$$\frac{\partial}{\partial t}\nabla^2\psi + J(\psi, \nabla^2\psi + f) = -\alpha\nabla^2\psi + F \tag{9}$$

where ψ is the geostrophic streamfunction, $J(a, b)$ is the Jacobian operator and F represents all processes not represented by the barotropic model.

We use the eigenvectors of a linearized version of Eq. (9) to establish one set of problem-dependent guess patterns. In contrast to the S-hierarchy, this set of patterns has the advantage of providing physically based suggestions for the mechanism of circulation changes. Due to the barotropicity it has the disadvantage of being limited to the non-tropical middle troposphere.

To derive the eigenvectors we follow Simmons et al. (1983) and Branstator (1985 a, b). After writing the state ψ as a sum of a mean state $\bar{\psi}$ and a perturbation $\psi'(t)$, $\psi = \bar{\psi} + \psi'$, and linearization, the following equation is obtained:

$$\frac{\partial}{\partial t}\psi' + M[\bar{\psi}]\psi' = F' \tag{10}$$

The matrix M arises from the Jacobians and the Ekman damping in (9) and is readily calculated using pseudo-spectral methods, as suggested by Simmons et al. (1983). The notation $M[\bar{\psi}]$ indicates that the matrix M depends on the mean state $\bar{\psi}$.

The matrix M has (complex) eigenvalues λ_j and eigenvectors e_j. Each state ψ' and F' may be expressed by the eigenvectors.

$$\psi' = \sum_j a_j \cdot e_j$$
$$F' = \sum_j f_j \cdot e_j \tag{11}$$

with the coefficients

$$a_j = d_j^t \cdot \psi' / d_j^t \cdot e_j$$
$$f_j = d_j^t \cdot F' / d_j^t \cdot e_j \tag{12}$$

The vectors d_j^t are the adjoint vectors of the e_j (i.e., $M^t d_j = \lambda_j^* d_j$) that form a biorthogonal basis such that $d_j^t \cdot e_i = 0$ if $i \neq j$. Inserting these expressions into (10), we find as the stationary response ψ' to the anomalous forcing F'.

$$\psi' = \sum_j \frac{1}{\lambda_j} f_j \cdot e_j \tag{13}$$

The response is stationary if the eigenvalues have positive real parts. It turned out that a damping rate of $\alpha = 1/10$ days^{-1} was sufficient to guarantee that all eigenvalues had positive real parts.

In view of the above consideration, it appears reasonable to use the eigenvectors e_j to guess the response of the GCM experiment. To do so, the eigenanalysis is done in the R11 (antisymmetric modes only) spectral space. The mean state $\bar{\psi}$ is specified by the geostrophic streamfunction in 300 hPa.

If we define $\bar{\psi}$ to be the average of two simulations (e.g., cold and warm or warm and control), (10) is formally equivalent to an anomaly general circulation model (Navarra and Miyakoda 1988; Schneider 1988). If $\bar{\psi}$ is the average of only one experiment, (10) is formally a perturbation GCM experiment with the chosen basic flow being disturbed by the anomalous boundary conditions.

The remaining question is how to define an adequate hierarchy. The most important patterns are associated with large coefficients $a_j = -\frac{f_j}{\lambda_j}$. Clearly the optimal choice of the pattern would be obtained by ordering the patterns by the weights: $\frac{f_1}{\lambda_1} > \frac{f_2}{\lambda_2} > \ldots$ Unfortunately, the forcing is not known. The connection between anomalous SST and anomalous vorticity forcing F' at 300 hPa is highly nonlinear and complex. Another ordering would be $\|d_1\| > \|d_2\| > \ldots$: If d_j is large, then one can expect f_j to be large also. We tried this approach and found that is was not succesful.

The finally ordering chosen

$$\|\lambda_1\| < \|\lambda_2\| < \ldots \tag{14}$$

is based almost solely on the imaginary (frequency) part of the eigenvalue. Those gravest modes are considered to be most probably affected by stationary forcing.

Thus, the barotropic normal mode "B-hierarchy" is defined by the sequence of eigenmodes of a specified basic flow $\bar{\psi}$ ordered according to the modulus of their respective eigenvalues. This hierarchy is similar to the one used by Hannoschöck and Frankignoul (1985), but

differs in one essential aspect: they used a zonally averaged mean state whereas we use a zonally asymmetric mean state.

Hierarchy A: normal modes of the temperature advection model.

Egger (1977) suggested that the atmospheric response to midlatitude SST anomalies is mostly confined to the lower troposphere and that the additional heating Q is balanced mainly by horizontal advection and an diffusive eddy transport:

$$\frac{\partial}{\partial t} T = -J(\psi, T) + \varepsilon \nabla^2 T + Q \tag{15}$$

A similar concept is that of the "advective limit" proposed by Webster (1981). Defining as above a mean $\bar{T}$ and an anomaly T', we get the following model for the anomaly

$$\frac{\partial}{\partial t} T' = -J(\bar{\psi}, T') - J(\psi', \bar{T}) + \varepsilon \nabla^2 T' + Q' \tag{16}$$

Since no à priori information on $J(\psi', \bar{T})$ is available, this term must be dropped. The model (16) cannot explain stationary solutions for the hemispheric-averaged temperature anomaly unless the area-averaged anomalous heating is zero, neglecting heat fluxes across the equator. Consequently, we must again drop the ψ_1^0 mode. Then (16) is formally identical to (10) and the guess patterns are chosen to be the eigenvectors of a matrix $M[\bar{\psi}]$, which is derived from the advection and diffusion terms in (16). The same principle that led to the B hierarchy is used to define the A hierarchy, i.e., the modes are ordered according to the modulus of the eigenvalues. The mean flow at 1000 hPa is used to specify $\bar{\psi}$. The diffusion coefficient ε is set to 100 m^2/s.

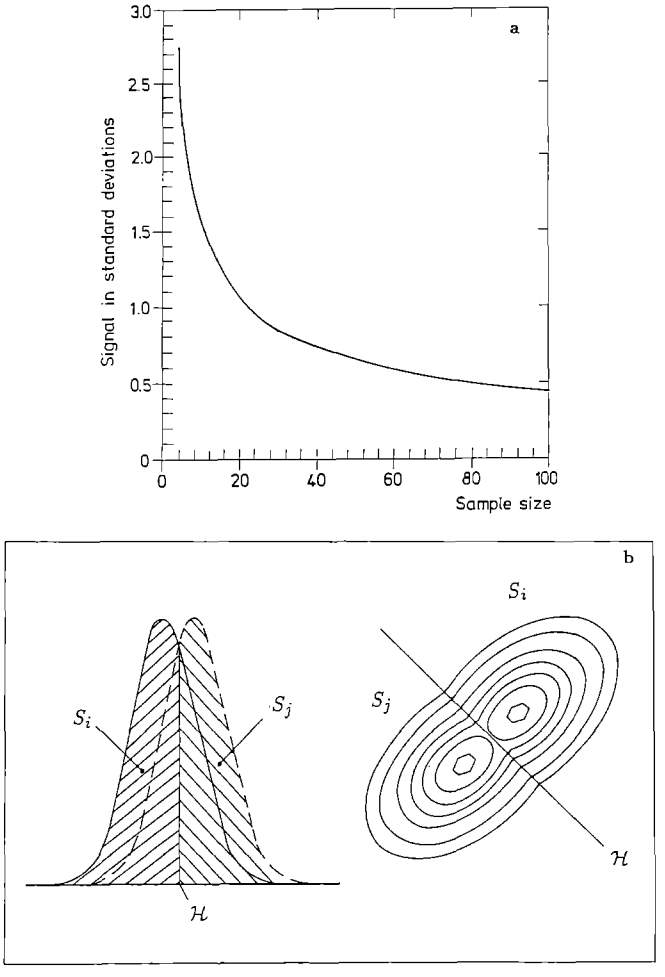

Fig. 5a, b. On the concept of recurrence. **a** Minimum difference of means, in units of standard deviations, which is identified by a t-test with a probability of at least 90% if the sample size of both ensembles increases (*horizontal axis*). **b** Schematic diagrams to illustrate the subdivision of the d-dimensional space into two complementary sets, S_i and S_j with $S_i \cup S_j = R^d$. *Left:* $d=1$; the *curves* show the probability densities. The $d-1=0$ dimensional hyperplane $\varkappa$ is a point on the horizontal axis. *Right:* $d=2$, contour plot of the probability densities. The 1-dimensional hyperplane $\varkappa$ is the straight line. After von Storch and Zwiers (1988) and Zwiers and von Storch (1989)

Analysis of the "warm versus cold" experiment

Technical details

The GCM output variables investigated were daily values of the spherical harmonic coefficients of the geopotential height at 300, 500 and 850 and 1000 hPa, the last one derived from SLP. With the help of the linear balance equation, the geostrophic streamfunction was derived. The low level temperature was approximated by the 850 hPa over 1000 hPa thickness: $T' \alpha (\psi(850\text{ hPa}) - \psi(1000\text{ hPa})) = \Delta_{850,1000}\, \psi'$.

From these daily values, geostrophic stream function and lower-level temperature, 30-day averages were formed. The first 30 days were omitted to avoid initial transients. Adjacent 30-day periods were separated by 10-day periods in order to obtain approximately independent realizations of a mean January climate. A 10-day gap was chosen as a trade-off between sufficient independency and a sufficient sample size.

This procedure resulted in two sets of size 17 "warm" and "cold" monthly means that form the samples on which to perform the statistical analysis in the three hierarchies, S, B and A. For the barotropic mode B-hierarchy the mean flow at 300 hPa, averaged over the warm and the cold experiment, is used (Fig. 6a). Similarly, the mean stream function at 1000 hPa, averaged over the two experiments, serves as $\bar{\psi}$ in the A-hierarchy (Fig. 6b).

Once a significant model is identified in the hierarchy (maximum number of parameters with risk less than 10% and level of recurrence $>80\%$), its mean difference is projected back into grid-point space to obtain a statistically filtered version of the response. This will be called the significant and recurrent pattern. The multivariate analysis was performed in the low-dimensional subspace spanned by the guess patterns. Therefore, the grid point representation of the significant and recurrent signal must not be interpreted locally. To allow for regional assessment of the signal's statistical stability, an additional local recurrence analysis is performed.

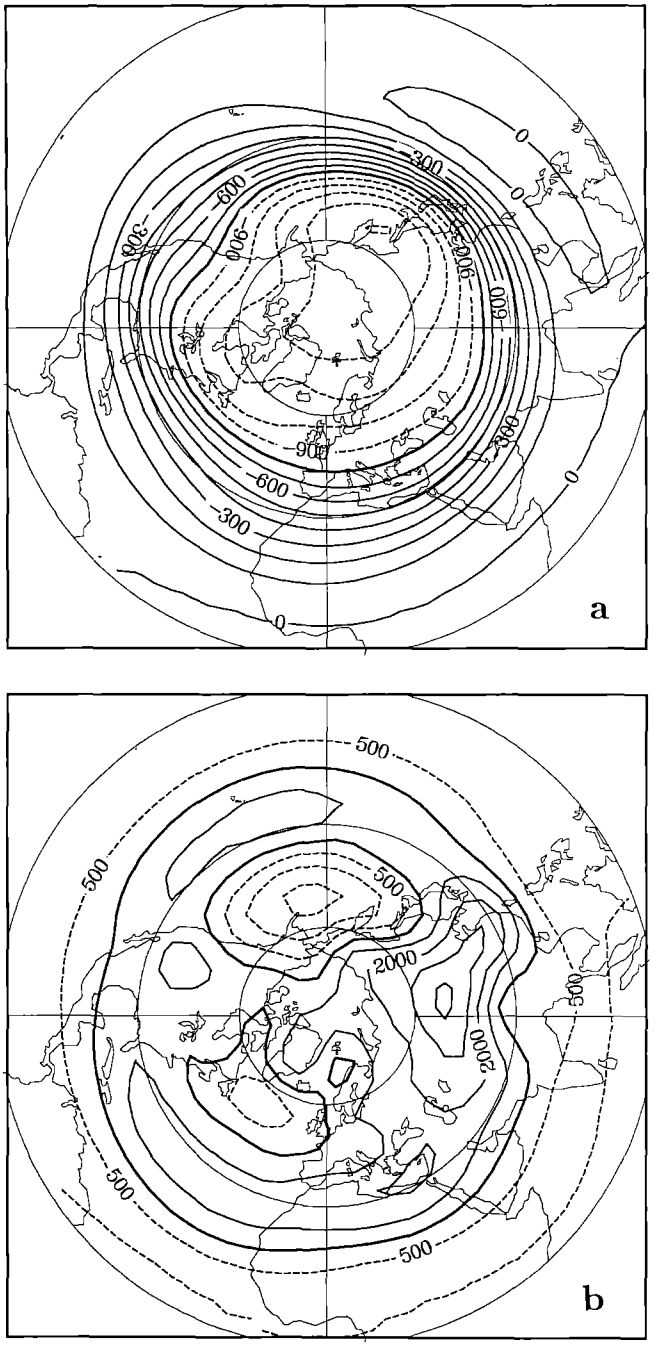

Fig. 6a, b. Long-term average geostrophic stream function in the warm and cold experiment. **a** 300 hPa: the mean flow to derive the barotropic normal modes of the B hierarchy; units m^2/s; contour interval 10^7 m^2/s. **b** 1000 hPa: the mean flow to derive the temperature advection normal modes of the A hierarchy; units m^2/s, contour interval 5.0 10^6 m^2/s

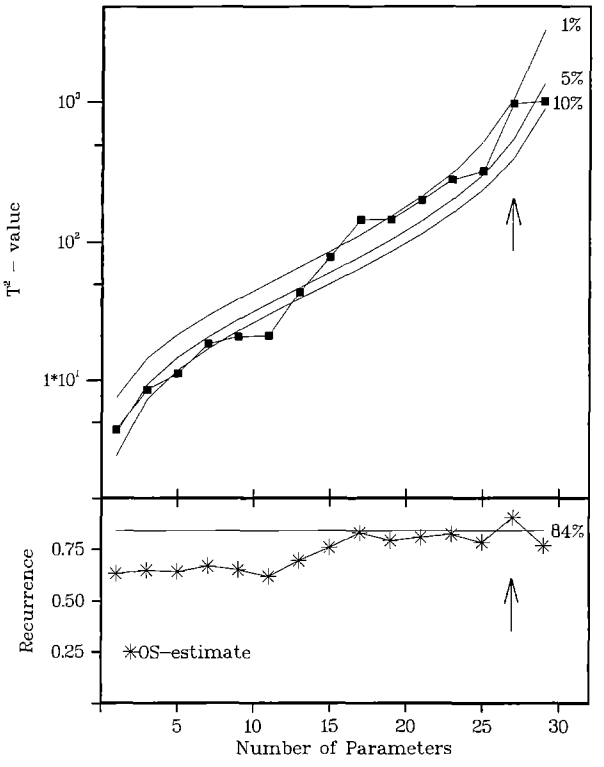

Fig. 7. Test statistic T^2 (*top*) and estimate of recurrence (*bottom*) as a function of A hierarchy parameters for the 850/1000 hPa layer temperature in the "cold vs warm" experiment. The *continuous lines* in the *top panel* are the indicated error levels for T^2 if the null hypothesis holds. The *arrow* marks the model selected as being "significant and recurrent"

Results

The results of statistical analysis of the "cold versus warm" experiment are summarized in Table 1.

Low-level temperature. As an example, the risk of the statistical test and the estimated level or recurrence are displayed in Fig. 7 as a function of the level of the hierarchy for 850/1000 hPa layer temperature in the A-hierarchy. Only odd parameter numbers enter the diagram because one stationary mode ($Im(\lambda_k)=0$) contributes to the hierarchy with one degree of freedom whereas all other modes add two parameters each [see Simmons et al. (1983) and Branstator (1985a, b)]. The model eventually chosen has 27 parameters. At this number of parameters the risk of falsely rejecting the null hypothesis is less than 5% and the level of recurrence is clearly maximum. An alternate choice could have been 17 parameters, yielding a model of less than 1% error level and 80% level of recurrence.

The 850/1000 hPa layer temperature $\Delta_{850,1000}\psi$ contains a significant and recurrent signal in both applicable hierarchies A and S (see Table 1). In Fig. 8 the reconstructed A and S signals are shown together with the full signal and the level of local recurrence. The A signal describes much more detail than the S signal, which is restricted to very large-scale guess patterns. With respect to "cold" cooling of the Atlantic-Eurasian hemisphere (30° W–150° E) and warming in the Pacific hemisphere are observed. Additonally, there are various small-scale features, many of which reflect weather noise and random sampling. The same large-scale feature is present in the two filtered maps as well. The S and A signals also correspond largely with respect to details. In the cold experiment, the lower troposphere over the eastern North Atlantic and most of midlatitude Eurasia was cooler than in the warm experiment. Si-

Table 1. Summary of the statistical analysis of the "cold vs warm" experiment using the hierarchies S, B and A. LH, Level of hierarchy which is identified as being significant and recurrent (=number of modes); R, risk=probability of equal means; LR, level of recurrence=probability of correctly classifying one sample as being from the warm or the cold experiment; EV, part of the total signal's variance explained by the significant and recurrent signal (%), – indicates that the hierarchy is not applicable and numbers in parentheses that the signal is significant but its estimated level of recurrence is less than 80%

Variable	Hierarchy S				Hierarchy B				Hierarchy A			
	LH	R	LR	EV	LH	R	LR	EV	LH	R	LR	EV
Stream function												
1000 hPa	23	5%	81%	75%			—				—	
850 hPa	(10	5%	70%	45%)			—				—	
500 hPa	(10	5%	70%	46%)			—				—	
300 hPa	7	1%	75%	55%	(11	5%	70%	45%)			—	
850/1000 hPa layer temperature	12	10%	74%	51%			—		27	5%	90%	46%

multaneously, there is a positive anomaly over midlatitude Pacific and North America, with a maximum situated over eastern Canada.

The high local recurrence levels indicate a stable temperature change over the eastern Atlantic and over Europe. The probability of negative temperature anomalies over the midlatitude Atlantic or Central Asia appearing in an individual January mean in another January simulation with "cold" Atlantic SST is estimated to be up to 85% or more when we compare it with the existing "warm" ensemble.

Stream function. A significant and recurrent signal is identified in the S hierarchy at 1000 hPa and in 300 hPa (Table 1). The signals at 850 hPa and 500 hPa are significant at the 5% error level, but the level of recurrence is only 70%. The same holds for the barotropic eigenmode hierarchy at 300 hPa where the recurrence level is always less than 70%. Therefore, only the signals at 1000 and 300 hPa are shown in Figs. 9 and 11.

The S-filtered signal at 1000 hPa picks up roughly 75% of the total field variance of the raw signal "cold vs. warm". The S reconstruction shown in Fig. 9a exhibits basically wave number 1 response: a positive anomaly has developed over and downstream of the cooler Atlantic SST with an opposite response for continuity reasons in the remaining part of the hemisphere. The local stability analysis (Fig. 9b) results in a fairly patchy pattern with maximum P values of 88%.

The low-level temperature and stream-function anomaly are synoptically consistent. The anomalous anticyclonic flow over the North Atlantic is connected with a southeasterly wind anomaly in the western part of the ocean, advecting anomalously warm maritime air masses to the cold land while a northerly wind anomaly in the European sector leads to negative temperature anomalies in that area.

The upper-level signal (S-hierarchy) (Fig. 11) at 300 hPa is considerably different form the low-level signal. In the cold simulation a dipole over North America indicates a reduced jet over the East Coast of the U.S. and an intensified zonal flow over the Atlantic. At the same time the Asian jet appears to be strengthened in the cold run. The univariate recurrence analysis suggests that both features are stable, in particular with respect to the meridional gradient over North America ($q=85\%$).

Discussion

In the Introduction we questioned if the observed decadal changes of SST were real and, if so, whether the simultaneously observed changes of the atmospheric circulation can be understood in part as an atmospheric response to the altered Atlantic SST. To answer these questions tentatively on the basis of our experiment we have to compare the model results with observations. For practical reasons, i.e., data availability, we have to limit this verification to SLP or the 1000 hPa stream function.

From the SLP observations a significant and recurrent pattern (5% and 80%) can be established for the difference in the average January fields between 1904–1913 and 1951–1960 (Fig. 3). This is based on the same methods as presented above except that we used as a hierarchy the regional EOFs of the Atlantic-European sector estimated from all January fields between 1881 and 1984. Comparison with the simulated ψ_{1000} pattern (Fig. 9) yields a gross similarity: in both maps there are two maxima over the midlatitude Atlantic and Western Europe and anomalous westward flow north of approximately 60° N. The regional data EOF hierarchy used to derive the observed signal can also be applied to the simulated SLP fields in the Atlantic European sector. In this case we find a significant and recurrent signal in the difference between cold and warm (1% and 78% using 10 EOFs). The reconstructed pattern is shown in Fig. 10. The comparison reveals that the simulated pattern is shifted relative to the observed pattern by about 30° of longitude to the east, and by about 10° to the north.

When comparing the simulated field and the observed changes we keep in mind that:

1. The model is not perfect in reproducing climatology in the Atlantic sector and with respect to the North Atlantic Oscillation (Glowienka-Hense 1988).

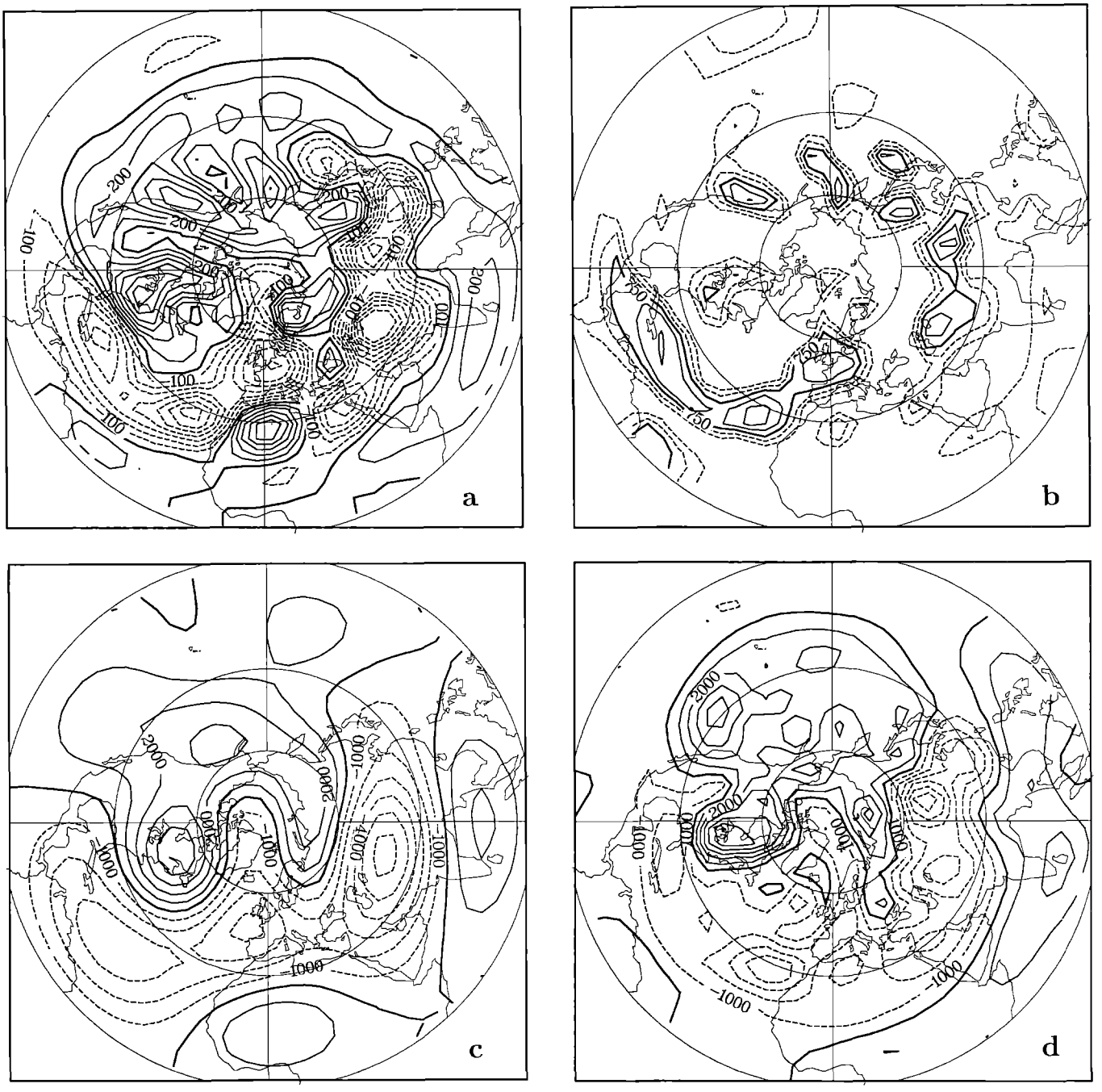

Fig. 8a–d. 850/1000 hPa layer-temperature signal in the "cold vs warm" experiment. **a** Total difference field; units m^2/s; contour interval 10^5 m^2/s. **b** Level of local recurrence *p*; $P=77$ (84)% corresponds to $q=93$ (98)% in von Storch and Zwiers (1988) and Eq. (5); units %; contour interval 5%; bold contour 75%. **c** "Significant and recurrent" signal in the S hierarchy; contour interval as in **a**. **d** "Significant and recurrent" signal in the A hierarchy; contour interval as in **a**

2. The imposed SST anomaly in the Atlantic is probably part of a global anomaly (Folland et al. 1986); thus the response in SLP in the Atlantic-European region could change if for example, North Pacific anomalies are also introduced.
3. We disregard the annual cycle by the perpetual January conditions; thus, the model response to a steady anomalous forcing in a steady background field could be different from that in a seasonal varying climatology.

In view of these limitations, we conclude that the GCM largely reproduces the atmospheric changes observed as a response to modified Atlantic SST, at least in terms of low-level circulation and temperature.

We anticipated two more questions that would be asked if a significant signal were to be identified, namley, about the signal's three-dimensional structure and the possibility of explaining part of the signal in terms of simplified theory.

The statistical analysis identified stable signals in

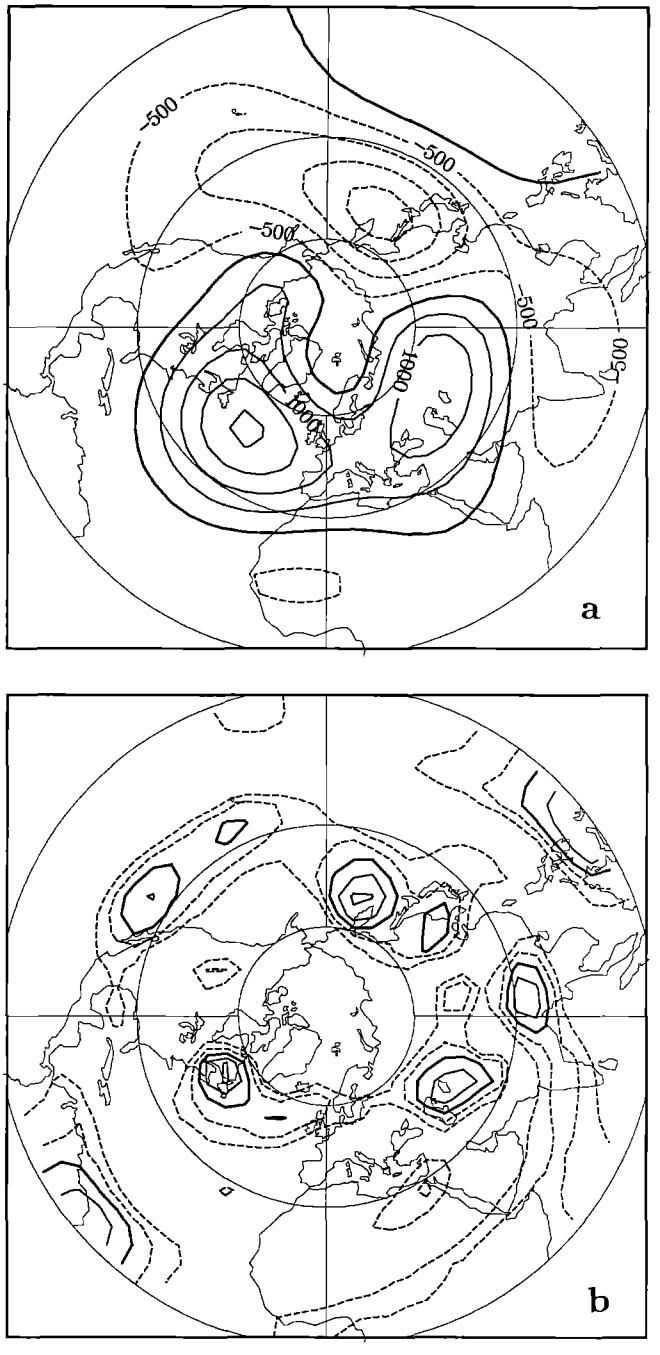

Fig. 9 a, b. 1000 hPa stream-function signal in the "cold vs warm" experiment. **a** "Significant and recurrent" signal in the S-hierarchy, units m^2/s, contour interval 5.0 10^5 m^2/sec; 1.5 10^6 m^2/s correspond to 2 hPa; **b** level of local recurrence p, $P=77$ (85)% corresponds to $q=93$ (98)% in von Storch and Zwiers (1988) and Eq. (5), units %, contour interval 5%; bold contour 75%

the S hierarchy at 1000 and 300 hPa (Figs. 9a and 11a) and less well-defined signals at 500 and 850 hPa (not shown). Figure 12 displays the meridional average of the S-filtered stream function anomalies within three zonal belts: low, middle and high latitudes. The structure of the signal at low levels differs strongly from that at upper levels. The near-surface level anomalies, between 850 and 1000 hPa, rarely exceed 10^6 m^2/s in the Atlantic-European region and the response in that region (Fig. 12b) appears to be local and shallow. Within the high latitude strip where no local forcing exists the response is restricted to the upper layers. The upper tropospheric response, however, appears to be out of phase or unrelated to the surface anomalies. This is most pronounced in the low latitude belt but also visible in the middle- and high-latitude strip with the exception of the Pacific region.

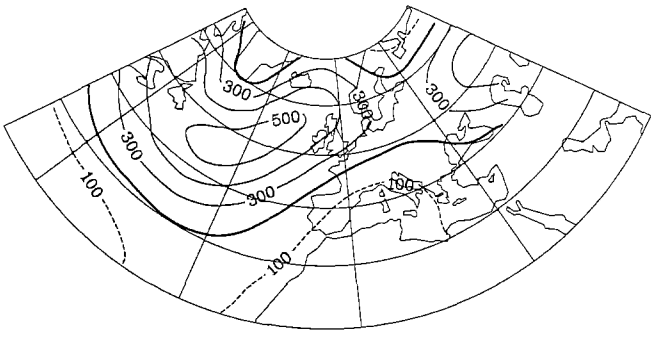

Fig. 10. "Significant and recurrent" sea level pressure signal in the "cold vs warm" experiment applying the data EOF hierarchy used in Fig. 3, units 10^{-2} hPa, contour interval 1 hPa, negative contours dashed

Thus the vertical structure of the signal in the extratropics can be described as a two-layer response of the lower troposphere (1000 and 850 hPa) against the upper troposphere (500 and 300 hPa). We suggest two possible explanations for this result.

1. The "baroclinic" hypothesis: the additional local heating from the ocean excites a baroclinic atmospheric response in which upper and lower levels are coupled.
2. The "two mechanisms" hypothesis: at lower levels the extratropical anomalies are the local response to the thermal changes, whereas at upper levels we see the remote response to tropical flow anomalies, and upper and lower layers tend to be decoupled at midlatitudes.

We favor the "two mechanisms" hypothesis for several reasons. First, the notion of a baroclinic response to extratropical SST anomalies would conflict with many GCM experiments (e.g., Rowntree 1979), with the finding of Barnett et al. (1984) that Atlantic SST anomalies tend to excite only local and regional downstream atmospheric responses and also with the notion of the "advective limit" (Webster 1981). The latter is supported by the success of the A hierarchy based on the eigenmodes of the low-level temperature advection equation: about one-half of the low-level temperature response can be explained by the linear advection and diffusion of the anomalous heating, a result in line with Egger's (1977).

The failure of the B hierarchy (Table 1) was fairly unexpected for us, especially in view of the result presented next (linearity of the response). There appear to be several possible reasons for this:

1. The basic term leading to the B hierarchy is an inadequate description of the governing physics, i.e., the notion of the response being a small disturbance is

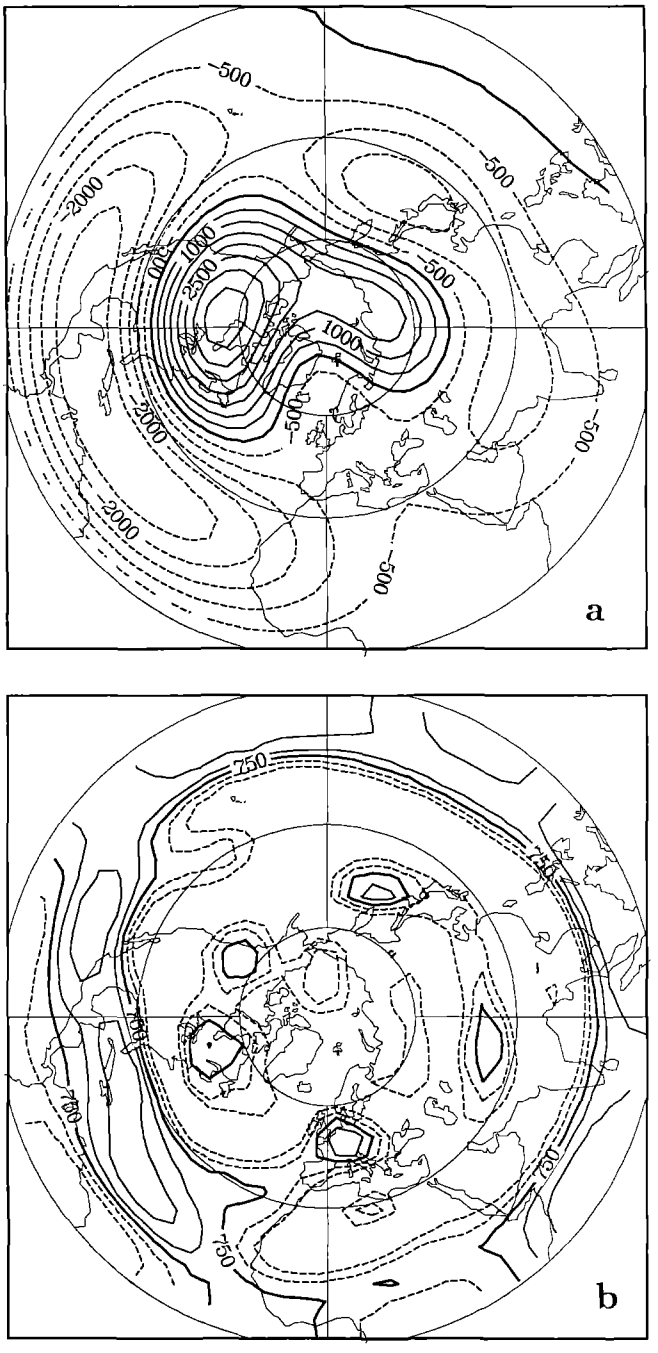

Fig. 11a, b. 300 hPa streamfunction signal in the "cold vs warm" experiment. **a** "Significant and recurrent" signal in the S-hierarchy, contour interval, units m^2/s, contour interval 5.0 10^5 m^2/s; **b** level of local recurrence p, $P=77$ (85)% corresponds to $q=93$ (95)% in von Storch and Zwiers (1988) and Eq. (5), units %, contour interval 5%; bold contour 75%

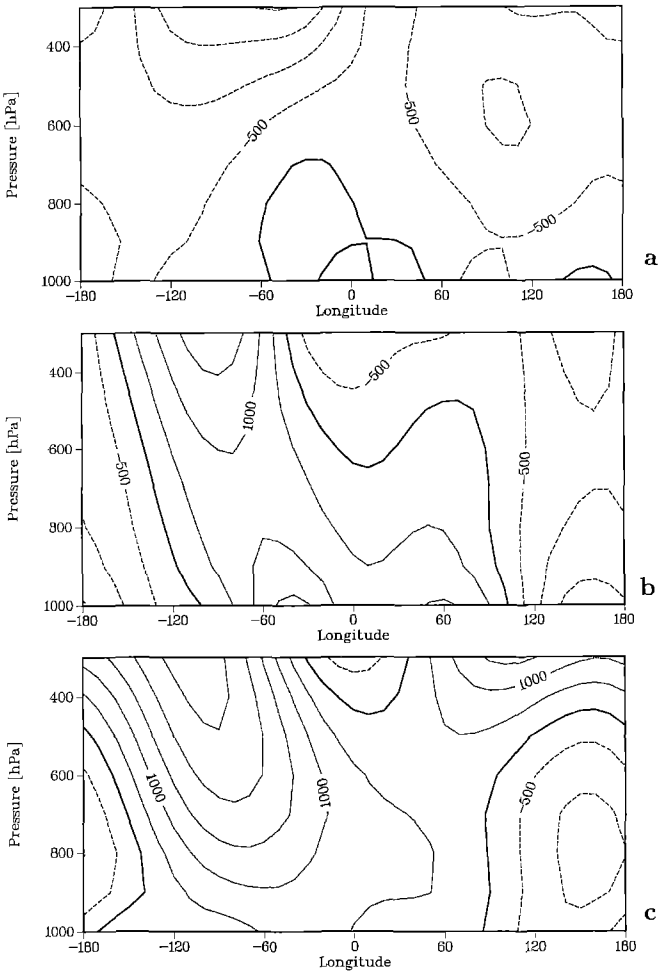

Fig. 12a–c. Meridional average, as a function of longitude and height, of the S-filtered streamfunction anomalies in the "cold vs warm" experiment units m^2/s, contour interval 5.0 10^5 m^2/s; **a** 0° N–30° N; **b** 30° N–60° N; **c** 60° N–90° N

not applicable. We will see that this is probably true.

2. The normal modes, and thus the result of the statistical analysis, depend strongly on the choice of the model parameters such as reported in Frankignoul and Molin (1988b). Deriving – as a sensitivity test – normal modes from all possible combinations of the mean flows, warm, cold and control, allowed us to reject this hypothesis. The eigenmodes, as well as the statistical results, are only marginally sensitive to the variations of the average flow, which may be understood as an à posteriori justification of the linearization.
3. The hemispheric formulation of the barotropic model (9) restricts all eigenmodes to be antisymmetric. Therefore, the model is of value only if only antisymmetric forcings are present. In particular, we have to expect the model to fail if strong disturbances of tropical heating, which are not symmetric to the equator, appear. To check this possibility, we analyzed the global distribution of 300 hPa velocity potential. Based on a global S hierarchy, we found a significant and recurrent signal in this quantity (Fig. 13). The pattern is certainly not very symmetric.
4. The quasigeostrophic formulation of the model completely ignores the advection of eddy vorticity by the mean divergent wind field, which has been shown to be of importance, especially in the subtropics (Sardeshmukh and Hoskins 1988; Held and Kang 1987).

For the sake of completeness we have to mention that we performed a sensitivity analysis for the A eigen-

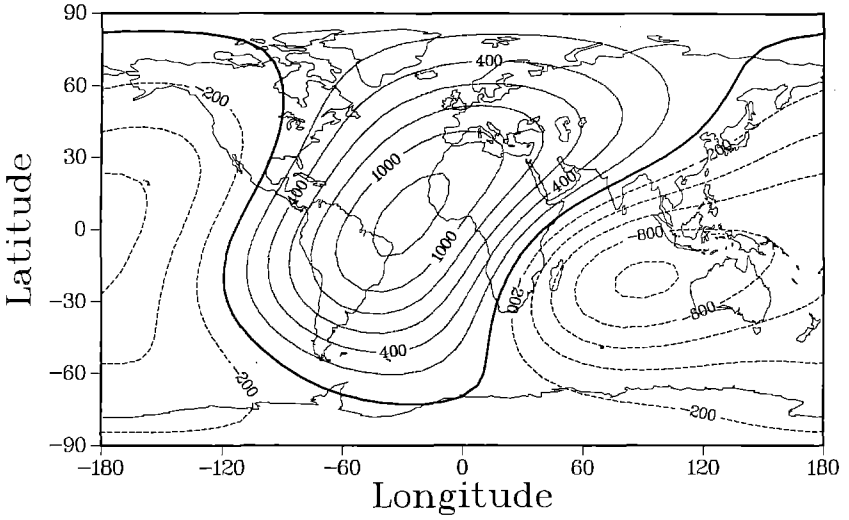

Fig. 13. Significant and recurrent signal form a global S hierarchy of the 300 hPa velocity potential in the "cold vs warm" experiment, units m^2/s, contour interval 2.0 10^5 m^2/s

modes as well. The statistical results are almost unaltered by moderate changes in the configuration of the basic flow $\bar{\psi}$. The sensitivity to the diffusion constant ε is such that an increase by two orders of magnitude decreases the significance and the level of recurrence but hardly alters the reconstructed variance.

An interesting question is whether our model results are in accord with the outcome of other GCM experiments on the effect of nontropical SST anomalies. We found a rising (lowering) of sea level pressure over and downstream the lowered (increased) SST. Similar behavior was found by Chervin et al. (1980), who considered the effect of subtropical and midlatitude SST anomalies in the Pacific. Using different versions of the GISS model, Hannoschöck and Frankignoul (1985) and Frankignoul and Molin (1988a, b) found conflicting responses to North Pacific SST anomalies, namely, either a response similar to ours or a nonsignificant low-level response. Palmer and Sun (1985) and Pitcher et al. (1988) simulated the effect of SST anomalies in the North Pacific and the North Atlantic and found a qualitatively different response, namely, negative, largely equivalent barotropic height anomalies downstream of negative SST anomalies, although in the latter two cases the imposed SST anomalies are about twice the amplitude of "cold vs warm".

The linearity of the response: analysis of the "warm vs control" and the "cold vs control" experiments

The third experiment "control" provides us with the possibility of studying the T21 response with respect to the strength of the imposed boundary changes. With respect to "control" both anomaly experiments, "warm" and "cold", operate with the same SST anomaly pattern. The strength of the SST anomaly pattern in the "cold" ("warm") experiment is about two-thirds (one-third) of the "cold vs warm" experiment. Therefore, the "warm" experiment is considered as being a "small disturbance" experiment and the "cold" as a "medium disturbance" experiment.

Low-level temperature

In the small amplitude disturbance experiment, "warm vs control", no signal is identified in both the S and the A hierarchies. In the "medium disturbance" experiment, a significant and recurrent signal appears in the A hierarchy but not in S. The A-filtered response patterns of the "cold vs control" and the "cold vs warm" experiments are very similar (not shown). We conclude that the low-level anomalous heating in our experiments is linear with respect to the imposed changes in SST and that the anomalous heating is balanced at low levels by anomalous advection.

300 hPa Stream function

Testing the response of the 300 hPa stream function to the small SST anomaly (warm vs control) yields a weak signal in the S hierarchy (risk: 10%; level of recurrence: 80%), which explains 45% of the total variance. The B hierarchy, however, leads to a considerable amplification of the signal, explaining more than 60% of the full signal, with a risk of 5% and a recurrence level of 90%. This result is insensitive to small variations in the basic flow. Both the B- and S-filtered pattern are broadly similar and only the B-dependent reconstruction is shown in Fig. 14a. It differs markedly from the significant and recurrent pattern identified in the "cold vs warm" experiment (Fig. 11), in particular over the Atlantic sector and over Asia. Concerning the tropical forcing mechanism, we also found a (weak) signal in a global S hierarchy for "warm vs control" in the 300 mb velocity potential. The reconstructed pattern (Fig. 14b) exhibits a monopole-like structure with anomalous outflow over the tropical Atlantic. The pattern is almost

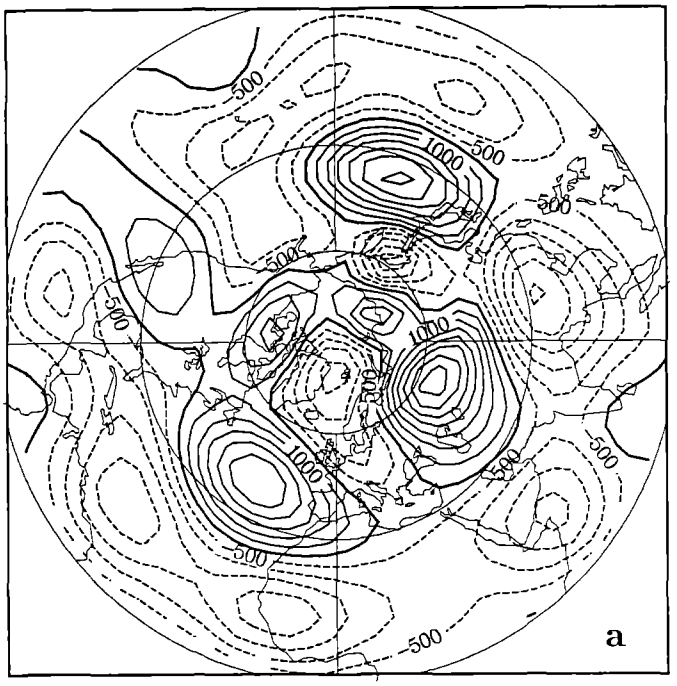

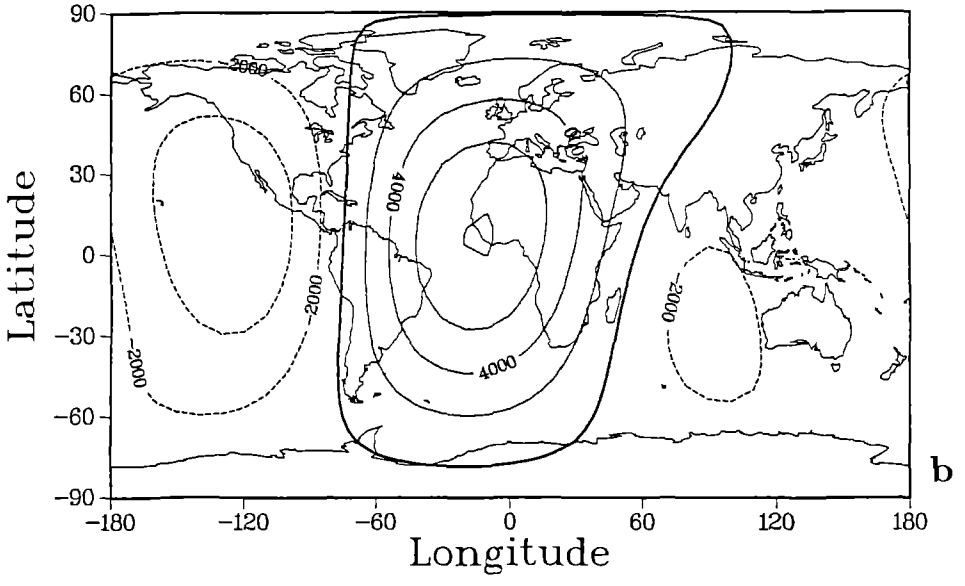

Fig. 14a, b. Results from the "control vs warm" experiment. **a** "Significant and recurrent" 300 hPa geostrophic streamfunction signal in the B-hierarchy, units m^2/s, contour interval 5.0 10^5 m^2/s; **b** "significant and recurrent" 300 hPa velocity potential signal in the S-hierarchy, units m^2/s, contour interval 2.0 10^5 m^2/s

symmetric to the equator, thus allowing mostly antisymmetric vorticity forcing.

The "cold vs control" signal appears weak in the S hierarchy (risk: 10%; level of recurrence: 75%). A significant and recurrent signal is identified in the B hierarchy (risk: 5%; level of recurrence: 81%). In contrast to the previous results, however, the latter result shows some sensitivity to the choice of the basic flow. Although this may introduce some arbitrariness in the interpretation, we present Fig. 15a for completeness. The B patterns (as well as the S-filtered patterns not shown) exhibit some similarity to the "cold vs warm" experiment. The tropical forcing, in terms of upper-air velocity potential (Fig. 15b), is very asymmetric.

From the performance of the B hierarchy in the three experiments, "cold vs warm", "cold vs control" and "warm vs control", we conclude that the upper-air stream-function response may be well represented by the linear barotropic model only in the "warm vs control" experiment, i.e., only the "warm vs control" SST anomaly leads to a "small disturbance", which would allow for the linearization of the physics. This is in contrast to the results for the lower layers and supports our "two mechanisms" hypothesis.

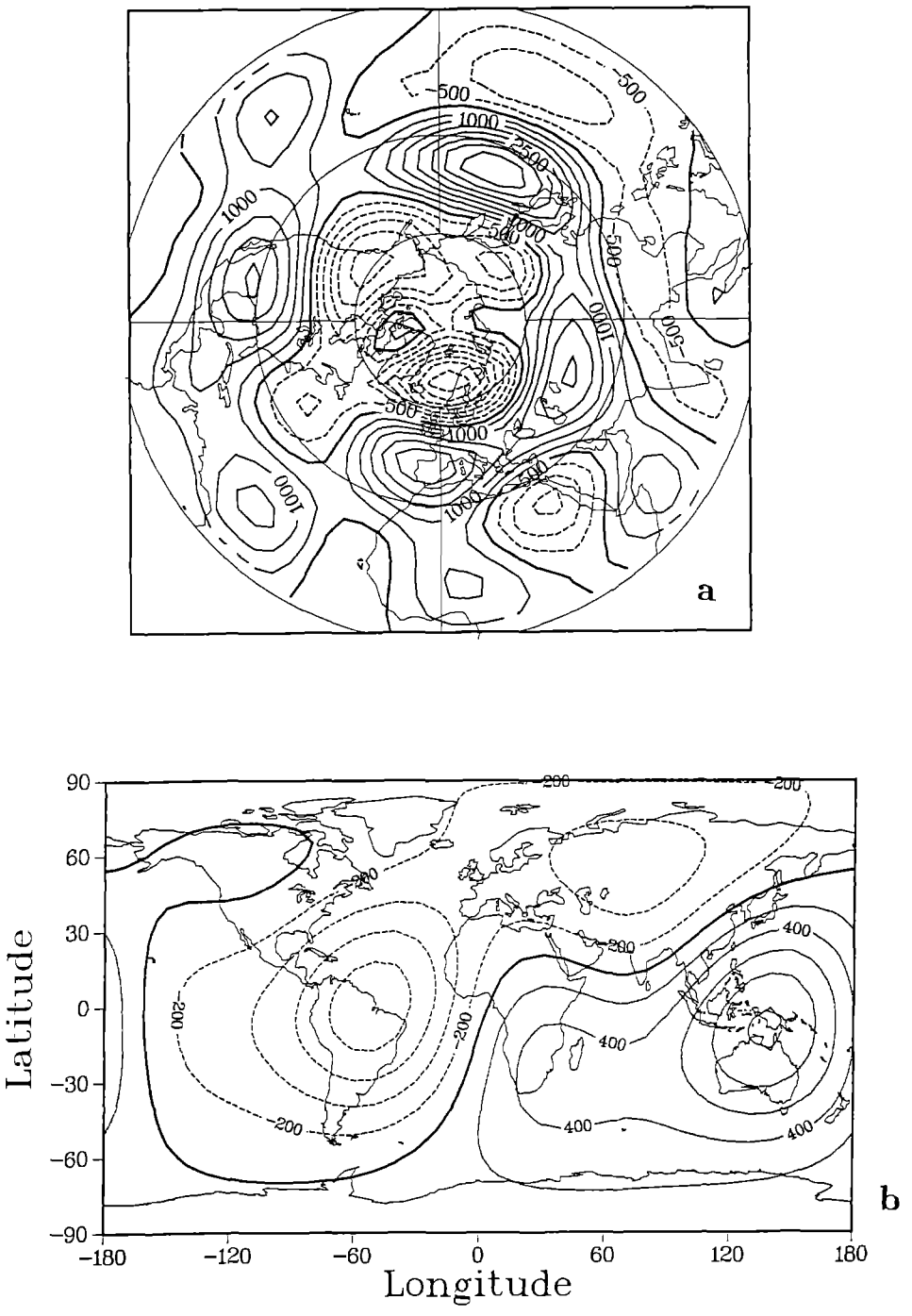

Fig. 15. Results from the "control vs cold" experiment. **a** "Significant and recurrent" 300 hPa geostrophic streamfunction, signal in the B-hierarchy, units m^2/s, contour interval 5.0 10^5 m^2/s; **b** "significant and recurrent" 300 hPa velocity potential signal in the S-hierarchy, units m^2/s, contour interval 2.0 10^5 m^2/s

Summary

We can make the following points regarding the modelled response to anomalous Atlantic SST:

1. The changes imposed in Atlantic SST lead to a change in surface pressure, which is in broad agreement with the observations. Thus, the observed decadal changes in SST are linked to atmospheric changes that were both observed and modelled. Certainly, the GCM used is not capable of delivering a reliable regional climatic "forecast". However, we are convinced that the model is capable of describing adequately an informed first guess of what the real changes might be.
2. The imposed midlatitude SST changes induce an anomalous surface heating, which is balanced by horizontal linear advection of the mean flow at 1000 hPa, thereby altering the low-level temperature structure of the GCM ("mechanism 1"). The relationship between imposed SST changes and temperature appears to be linear as far as one can see on the basis of three samples. This result is in agreement with the theoretical works by Egger (1977) and Webster (1981), the observational study by Barnett et

al. (1984) and with many GCM experiments (Rowntree 1979). It is in conflict with the GCM studies by Palmer and Sun (1985) and Pitcher et al. (1988) who found their GCMs to generate vertically penetrating responses to midlatitude SST anomalies. One could speculate that the latter results show the signature of a different regime since the SST anomalies of those two studies are of larger amplitude than those imposed in our experiments.

3. The response of the upper tropospheric flow seems to result from changes in the convective activity that are due to the imposed SST variations and in turn change the upper tropospheric divergence patterns. This acts as an anomalous vorticity forcing for the mean flow at 300 hPa. It initiates small, almost linear variations in the flow for the weak anomaly case "control vs warm" but apparently a more complex relationship for the stronger anomaly cases "control vs cold" and "cold vs warm" ("mechanism 2").

Acknowledgements. We are indebted to Harry van Loon (NCAR) for suggesting the GCM experiments. Dr. O. Höflich gave valuable comments on the quality of the HSST data set, and Ingo Jessel and Heiko Borgert helped us with processing the data. Finanical support was given by the "Klimaprogamm der Rheinisch-Westfälischen Akademie der Wissenschaften" under Prof. H. Flohn and from the Bundesministerium für Forschung und Technologie. Dr. Barbara Bruns gave valuable advice on the English.

References

Alexander RC, Mobley RL (1976) Monthly average sea-surface temperatures and ice-pack limits on a 1° global grid. Mon Weather Rev 104:143–148

Barnett TP, Preisendorfer RW, Goldstein LM, Hasselmann K (1981) Significance tests for regression model hierarchies. J Phys Oceanogr 11:1150–1154

Barnett TP, Heinz HD, Hasselmann K (1984) Statistical prediction of seasonal air temperatures over Eurasia. Tellus 36A:132–146

Branstator G (1985a) Analysis of general circulation model sea-surface temperature anomaly simulations using a linear model. Part I. Forced solutions. J Atmos Sci 42:2225–2241

Branstator G (1985b) Analysis of general circulation model sea-surface temperature anomaly simulations using a linear model. Part II. Eigenanalysis. J Atmos Sci 42:2242–2254

Chervin RM, Kutzbach JE, Houghton DD, Gallimore RG (1989) Response of the NCAR general circulation model to prescribed changes in ocean surface temperature. Part II. Midlatitude and subtropical changes. J Atmos Sci 37:308–322

Egger J (1977) On the linear theory of the atmospheric response to sea surface temperature anomalies. J Atmos Sci 34:603–614

Fischer G (ed) (1987) Climate simulations with the ECMWF T21 Model in Hamburg. Meteorologisches Institut der Unversität Hamburg. Large Scale Atmospheric Modelling Report 1

Folland CK, Palmer TN, Parker DE (1986) Sahel rainfall and worldwide sea temperatures 1901–85. Nature 320:602–607

Frankignoul C, Molin A (1988a) Response of the GISS general circulation model to a midlatitude sea surface temperature anomaly in the North Pacific. J Atmos Sci 45:95–108

Frankignoul C, Molin A (1988b) Analysis of the GISS GCM response to a subtropical sea surface temperature anomaly using a linear model. J Atmos Sci 45:3833–3845

Glowienka R (1985) Studies on the variability of Icelandic low and Azores high between 1881 and 1982. Beitr Phys Atmos 58:160–170

Glowienka-Hense R (1988) Performance of the ECMWF T21 model in simulating the North Atlantic oscillation (NAO). Climate simulations with the ECMWF T21-model in Hamburg, Part II. In: Storch H von (ed) Meteorologisches Institut der Universität Hamburg Large Scale Atmospheric Modelling Report 4:35–51

Hannoschöck G, Frankignoul C (1985) Multivariate statistical analysis of a sea surface temperature anomaly experiment with the GISS general circulation model. J Atmos Sci 42:1430–1450

Hasselmann K (1979) On the signal- to-noise problem in atmospheric response studies. Meteorology over the tropical oceans. R Met Soc London, pp 251–259

Held I, Kang I-S (1987) Barotropic models of the extratropical response to El Niño. J Atmos Sci 44:1433–1452

Hense A (1986) Multivariate statistical analysis of the Northern Hemisphere circulation during the El Niño 1982/83. Tellus 38A:189–204

Höflich W (1974) The seasonal and secular variations of the meteorological parameters on both sides of the ITCZ in the Atlantic ocean. GARP Report 2

Jones PD, Raper SCB, Santer BS, Cherry BSG, Goodess C, Bradley RS, Diaz HF, Kelly PM, Wigley TML (1985) A gridpoint surface air temperature data set for the Northern Hemisphere, 1851–1984. – DoE technical Report No. 22 US Department of Energy Carbon Dioxide Research Division, Washington DC, 251 pp

Lautenschlager M, Schlese U, Ponater M, Mai W, Ulbrich U, Speth P (1988) Atmospheric response to Ice Age January conditions. Climate Simulations with the ECMWF T21-model in Hamburg, Part II, H v Storch (ed) Meteorologisches Institut der Universität Hamburg Large Scale Atmospheric Modelling Report 4:191–230

Loon van H, Rogers J (1978) The seesaw in winter temperature between Greenland and northern Europe. Part I: General description. Mon Weather Rev 106:296–310

Loon van H, Madden RA (1983) Interannual variations of monthly mean sea-level pressure in January. J Climate Appl Met 22:687–692

Navarra A, Miyakoda K (1988) Anomaly general circulation models. J Atmos Sci 45:1509–1530

Okamoto M (1963) An asymptotic expansion for the distribution of the linear discriminant function. Ann Math Stat 34:1286–1301

Page JT (1985) Error rate estimation in discriminant analysis. Technometrics 27:189–198

Palmer TN, Sun Zhaobao (1985) A modelling and observational study of the relationship between sea surface temperature in the north-west Atlantic and the atmospheric general circulation. Quart J R Met Soc 111:947–975

Pitcher EJ, Blackmon ML, Bates GT, Munoz S (1988) The effect of North Pacific sea surface temperature anomalies on the January climate of a general circulation model. J Atmos Sci 45:173–188

Rogers JC (1985) Atmospheric circulation changes associated with the warming over the northern North Atlantic in the 1920s. J Climate Appl Met 24:1303–1310

Rowntree, PR (1979) The effects of changes in ocean temperatures on the atmosphere. Dyn Atmosph Oceans 3:373–390

Sardeshmukh P, Hoskins BJ (1988) The generation of global rotational flow by steady idealized tropical divergence. J Atmos Sci 45:1228–1252

Schneider EK (1988) A formulation for diagnostic anomaly models. Pageoph 126:137–140

Simmons AJ, Wallace JM, Branstator G (1983) Barotropic wave-propagation and instability, and atmospheric teleconnection patterns. J Atmos Sci 40:1363–1392

Storch H von, Kruse H (1985) The extratropical atmospheric response to El Niño events. Tellus 37a:361–377

Storch H von (1987) A statistical comparison with observations of control and El Niño simulations using the NCAR CCM. Beitr Phys Atmosph 60:464–477

Storch H von, Zwiers F (1988) Recurrence analysis of Climate sensitivity experiments. J Climat 1:157–171

Storch H von (ed) (1988) Climate simulations with the ECMWF T21-Model in Hamburg Part II: Climatology and sensitivity experiments. Meteorologisches Institut der Universität Hamburg Large Scale Atmospheric Modelling Report 4:265 pp

Webster PJ (1981) Mechanism determining the atmospheric response to sea surface temperature anomalies. J Atmos Sci 38:554–571

Zwiers F, Boer GJ (1987) A comparison of climates simulated by a general circulation model when run in the annual cycle and perpetual modes. Mon Wea Rev 115:2626–2644

Zwiers F, Storch H von (1989) Multivariate Recurrence Analysis. J Climat 2:1538–1553